Chemical Research in Toxicology

Article

Determination and prediction of the binding interaction between organophosphate flame retardants and p53

Fei Li, Xianhai Yang, Xuehua Li, Renmin Li, Jianmin Zhao, and Huifeng Wu

Chem. Res. Toxicol., **Just Accepted Manuscript** • DOI: 10.1021/tx5002157 • Publication Date (Web): 21 Oct 2014

Chemical Research in Toxicology is published by the American Chemical Society. 1155 Sixteenth Street N.W., Washington, DC 20036

Determination and prediction of the binding interaction between organophosphate flame retardants and p53

Fei Li [†*], Xianhai Yang [‡], Xuehua Li [‡], Renmin Li [§], Jianmin Zhao [†], Huifeng Wu[†*]

[†]*Key Laboratory of Coastal Zone Environmental Processes and Ecological Remediation, Yantai Institute of Coastal Zone Research (YIC), Chinese Academy of Sciences(CAS); Shandong Provincial Key Laboratory of Coastal Zone Environmental Processes, YICCAS, Yantai Shandong 264003, P. R. China;*

[‡]*Key Laboratory of Industrial Ecology and Environmental Engineering (MOE), School of Environmental Science and Technology, Dalian University of Technology, Linggong Road 2, Dalian 116024, P. R. China;*

[§]*Qingdao Institute of Bioenergy and Bioprocess Technology, Chinese Academy of Sciences, Qingdao 266101, Shandong, PR China.*

[*] Author for correspondence: Fei Li: Tel and Fax: +86-535-2109189, E-mail: fli@yic.ac.cn; Huifeng Wu, Tel: +86-535-2109190, E-mail: hfwu@yic.ac.cn.

Table of Contents (TOC) graphic

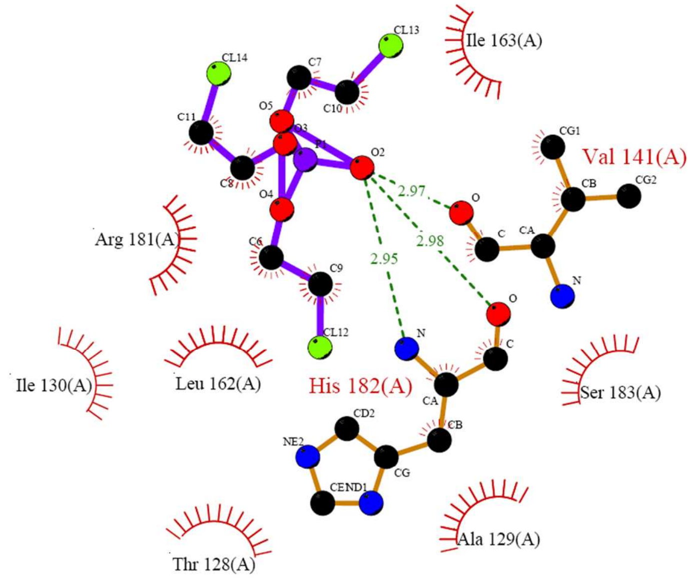

Abstract

The organophosphate flame retardants (OPFRs) have caused widely concerns because of the harm to environment. In this study, to better explain the mechanism for the OPFRs binding with the tumor suppressor genes p53, an integrated experimental and *in silico* approach was used. The binding constants of ten OPFRs were measured by surface plasmon resonance technology (SPR). The effect of OPFRs on p53 gene and protein expression in ZF4 cell were determined by quantitative Real-time PCR and western blotting. Molecular docking and dynamics simulation were explored to find that the H-bonds and hydrophobic interactions were the dominant interaction between OPFRs and p53. On the basis of the observed interactions, proper molecular structural descriptors were used to build the quantitative structure-activity relationship (QSAR) model. The current QSAR model was of robustness, predictive ability and mechanism interpretability. The applicability domain of the QSAR was discussed by the Williams plot. The results showed that H-bonds and electrostatic interaction govered the binding affinities between OPFRs and p53.

Key words organophosphate flame retardants (OPFRs); p53; docking; quantitative structure-activity relationship (QSAR); binding affinity; partial least squares (PLS)

1. Introduction

As a number of available alternatives to polybrominated diphenyl ethers (PBDEs), the usage of organophosphate flame retardants (OPFRs), such as the triesters tris-(2-chloroethyl)-phosphate (TCEP) and triphenyl phosphate (TPP), are currently widespread and expected to increase.[1] OPFRs could enter into the surroundings relatively easily because they are not covalently bound to host materials.[2,3] OPFRs are considered as re-emerging pollutants because of their vast use, and are considered to be persistent in the environment.[1]

The chlorinated alkylphosphates, such as tris(2-chloropropyl) phosphate (TCPP) and TCEP, are mostly added in polyurethane foam to be flame retardants.[4] The derivatives such as tri-*n*-propylphosphate (TPrP), tri-iso-butylphosphate (TiBP), triethylphosphate (TEP) and TPP are mainly used as plasticisers, lubricants and flame retardants. Many of them have been frequently detected in the environmental medium, including air,[5] indoor dust,[2,6,7] water,[8,9] sediments,[10] soils,[11] landfill leachates[12] and even in the aquatic organisms and in human breast milk.[13]

Limited studies suggest that certain OPFRs may be carcinogenic, neurotoxic, and/or reproductive toxicants.[14-16] It is suggested that TPP may inhibit the activity of monocyte carboxylesterase in human blood.[17] Meeker and Stapleton have reported that TPP in the dust can affect the semen quality.[18] However, more experiments are necessary to determine the potential risks after exposed to OPFRs.

Zebrafish have been an important model organism in genetics and in developmental biology.[19] Zebrafish can be subjected to chemical mutagens and thus many mutants can be produced quickly.[20] Comparison to the human reference genome, some genes of zebrafish have the highest homology with human (up to 70%).[21] Indeed, the zebrafish has been successfully utilized in genetic analyses, and libraries containing hundreds of mutants have

been established.

The tumor suppressor p53 can prevent the growth of cancer and maintain the stability of genom.[22,23] The correct conformation of the p53 DNA-binding domain plays an important role for target genes binding and transactivation. It is supposed that the interaction of OPFRs with the protein can disrupt the conformation of p53 DNA-binding domain. Therefore, it is of much necessity to reveal the mechanism of OPFRs binding interaction with p53.

Because of huge number of the compounds, it is of great attention on developing *in silico* methods to research the binding interaction between compounds and p53, such as quantitative structure-activity relationship (QSAR).[24,25] It is suggessted by the organization for economic co-operation and development (OECD) guideline, QSAR model development should following these principles: (i) a clear endpoint, (ii) an unambiguous algorithm, (iii) a defined applicability domain (AD), (iv) goodness-of-fit, robustness and predictivity, and (v) a mechanistic interpretation.[26] Then the current QSAR model on binding interaction of OPFRs to p53 followed these guidelines. Furthermore, molecular docking have become an important part of molucular structure-based computational simulations of chemicals.[27] Combinational use of molucular simulation with QSAR can get more information on the interactions between the OPFRs and the p53.[28-30]

Surface plasmon resonance (SPR) has been employed extensively in the field of DNA/DNA, DNA/protein, and small molecule protein/DNA interactions.[31-33] SPR was explored to monitor in real time the association and dissociation reactions in the ligand/receptor system. In the study, the binding interactions for OPFRs with zebrafish p53 protein were explored. The zebrafish p53 protein was expressed in *E.coli* and purified through denaturization and renaturation. The binding affinity of OPFRs to p53 protein was measured by SPR. The interaction between OPFRs and p53 were established by molecular docking analysis. Moreover, the theory prediction model for the binding constants of OPFRs

interacting with p53 was developed. The results could be conducive to understand the genetic mechanism for OPFRs compounds, and could provide the theory basis for their pollution prevention and control.

2. Materials and methods

2.1 RNA extraction and amplication

Total RNA was extracted from zebra fish using the TRIzol Reagent (Invitrogen, USA) following the manufacturer's protocol. In ordeer to remove DNA contamination, RQ1 RNase-Free DNase (Promega, USA) was added in the extracted RNA. The p53 cDNA fragments were amplified and cloned by reverse transcription and polymerase chain reaction method (RT-PCR) using p53-specific primers 5'-GACTATCCCGGCGATCATGGATT-3' and 5'- TTTCTTGAAGTTGCTCTCCTCAG-3'. M-MLV reverse transcriptase (Promega, USA) was used to synthesis the single-stranded cDNAs.

2.2 Recombinant expression, denaturing purification and renaturation of p53 protein

The pET28a expression vector (Novagen) was used to clone the final amplified product. The core DNA-binding domain of p53 was overproduced in *E. coli* BL21 (DE3). The cells were cultivated at 37 °C until the OD reached to 0.5-0.8. After that, 0.6 mM isopropyl β-D-thiogalactoside was joined to induce the expression of the recombinant protein at 25 °C for 6 h. All subsequent procedures were performed at 4 °C. The cells were harvested and washed and purified as previously described.[34]

2.3 Binding constants for OPFRs using biacore analyses

The interaction between p53 and OPFRs was measured by SPR on Biacore T100 (GE Healthcare) using the CM5 sensor chips employed at 25 °C. The zebrafish p53 DBD was immobilized on a CM5 chip. The CM5 sensor chip surface was activated by injection of

EDC/NHS (1:1) at 10 μL/min for 7 minutes, then injection of p53 in 10mM sodium acetate pH 5.0 at 10 μL/min for 7 minutes to immolize p53 on the CM5 sensor chip surface, deactivate excessive reactive groups using ethanolamine. The binding of OPFRs to the p53 was measured using HBS with 0.05% P20 and 5% DMSO as the running buffer (0.15 M NaCl, 10 mM HEPES, pH 7.4) at the flow rate of 30 ml/min. The sensor data were matched using Biacore T100 evaluation software. During the analysis of SPR, the association rate constant (k_a) and dissociation rate constant (k_d) are gained separately. And then, the dissociation constant (K_D) value can be calculated by k_d/k_a. More details could be found in the previous study.[35,36]

2.3 Quantitative Real-time PCR of p53 gene expression and western blotting analysis

Zebrafish embryonic fibroblast (ZF4) cells were kindly provided by Professor Xiaoming Hang in Dalian Maritime University and maintained in Dulbecco's modified Eagle's medium and Ham's F-12 (DMEM/F12), added with 10% (v/v) fetal bovine serum (FBS), 100 U/ml penicillin, and 100 μg/ml streptomycin, in a humidified atmosphere containing 5% CO_2 at 28 °C.

The ZF4 cells were exposed with low, media and high concentration (10^{-6}, 10^{-5}, 10^{-4} M) of TCEP or TPhP for 24 h, respectively. Total RNA was isolated in TRIzol reagent (Invitrogen, Carlsbad, CA, USA) from the ZF4 cells following the manufacturer's directions. RT-PCR primers used to quantify the β-Actin and p53 are Forward-CGAGCAGGAGATGGGAACC, Reverse-CAACGGAAACGCTCATTGC, Forward-GGGCAATCAGCGAGCAAA and Reverse-ACTGACCTTCCTGAGTCTCCA. The RT-PCR were implemented in a total volume of 25.0 μl containing 4.0 μl of 1 : 20 diluted cDNA, l.0 μl of each primer, 12.5 μl of 2

× SYBR Green Master Mix, and 6.5 μl of PCR-grade water in triplicate. The PCR program was started at 95 °C for 10 min, followed by 40 cycles for 30 s at 95 °C, 20 s at 60 °C, and 1 min at 72 °C. The last cycle was 95 °C for 35 s, 60 °C for 25 s, and 72 °C for 10 min. After that, data were analyzed with the ABI 7500 SDS software. The expression levels of p53 gene were calculated by the comparative CT ($2^{-\Delta\Delta CT}$) as previously described.[37]

The extracted protein sample of each group was subjected to 12% SDS-PAGE and transferred onto the polyvinylidene fluoride membrane (PVDF) for western blotting. After incubated by the primary and secondary antibodies, DAB Horseradish Peroxidase Color Development Kit was employed to detect the expression of p53. And then, the Gel-pre 4 software was used to quantify the protein band intensities.

2.4 Homologous modeling and molecular docking for the binding interaction

From the similar sequence searching with BLAST, the amino acid residue sequence of p53 conservative domain was obtained and the sequence alignment was completed by ClustalW. The homologous three dimision model of p53 DNA binding domain was generate on the SWISS-MODEL net server. The binding interactions were simulated by the Discovery Studio 2.5 (Accelrys Software Inc.) through the CDOCKER protocol, which is an docking tool based on the CHARMm force field.[38] Through dynamics simulation, random ligand conformations are generated. The mechanism of the intermolecular interaction can be obtained by the moleuclar simulation.

2.6 Molecular Dynamics Simulation

The MD simulation were carried out with Discovery Studio 2.5 through the Simulation protocol. The CHARMM27 force field was defined to the compounds by using Apply

Forcefield protocol. The ligand-recptor complex was solvated in a water molecules box, and the boundary of the box is at least 7 Å away from any atoms. The whole systems were then energetically minimized by the steepest-descent method. The obtained minimized systems were heated from 50 to 300K for 50 ps at a constant volume, restrainting the ligands. The heated systems were equilibrated at 300K for 500 ps, restrainting the ligands. The MD simulation were then performed in the NPT ensemble with periodic boundary conditions. Using the particle mesh Ewald (PME) algorithm, the electrostatic and van der Waals interactions were calculated.

2.7 Molecular structural descriptor selection

As suggested by the OECD guideline,[26] QSAR should be built on the basis of the mechanism. The binding activities could depend on: (a) the partition ability in the bio-phase, and (b) The hydrogen-bond or electrostatic interactions. The chemical structures were obtained by CS Chem3D Ultra (Version 6.0). $\log K_{\mathrm{OW}}$ was chosen to express the partition ability and hydrophobic interaction. The parameters V, μ, $HATS_{0\mathrm{m}}$, $RDF_{030\mathrm{v}}$, $X_{5\mathrm{A}}$, $MATS_{8\mathrm{v}}$, $MATS_{7\mathrm{v}}$, $RDF_{035\mathrm{m}}$ and $Mor_{17\mathrm{m}}$ also partly described the partition since many of these parameters correlate with $\log K_{\mathrm{OW}}$.[39] The parameters E_{HOMO}, E_{LUMO}, q_{PQ}, q^-, ω, μ, η, $E_{1\mathrm{e}}$ and $MATS_{8\mathrm{e}}$ were chosen to show the hydrogen bond or electrostatic interactions between the OPFRs and p53. The descriptors such as E_{HOMO}, E_{LUMO} and q^- had been used in some QSAR models for representing the intermolecular electrostatic interactions.[40]

$\log K_{\mathrm{OW}}$ values were obtained from Reemtsma et al.[3] The quantum chemical parameters were obtained by the Gaussian 09 programs.[41] The initial geometries of the OPFRs were optimized at B3LYP/6-31G(d, p) level through the hybrid Hartree-Fock density functional

theory.[42] Water was used as solvent, the polarized continuum model (IEFPCM) was used to consider the effect of water.[43] The frequency analysis was also operated to make sure that there were no imaginary vibration frequencies. $HATS_{0m}$, RDF_{030v}, X_{5A}, $MATS_{8v}$, E_{1e}, $MATS_{7v}$, $MATS_{8e}$, RDF_{035m}, and Mor_{17m} were calculated by the DRAGON software.[44]

2.8 The development, validation and AD of QSAR Model

The 10 OPFRs were randomly splited to a training set (70%) and a validation set (30%), (Table 2). The QSAR model was built by partial least squares (PLS) regression embeded in Simca-S because it can avoid strongly collinear and noisy during the analysis of data.[45] The leave-many-out cross validation was performed to obtain the number of PLS components (A). Through the cross-validation, a statistical Q^2_{CUM} (the fraction of the total variation of the dependent variables that can be predicted by all the extracted components) for model was obatained to evaluate the QSAR model.[28,29] The external validation was pereformed to assess the predict ability of the model. These parameters, the determination coefficient (R^2), root mean square error (*RMSE*) and external explained variance (Q^2_{EXT}), were calculated to characterize the model performance as following:[46]

$$R^2 = 1 - \sum_{i=1}^{n}(y_i^{\mathrm{fit}} - y_i)^2 \Big/ \sum_{i=1}^{n}(y_i - \bar{y})^2 \qquad [1]$$

$$RMSE = \sqrt{\sum_{i=1}^{n}(y_i - \hat{y}_i)^2 \Big/ n} \qquad [2]$$

$$Q^2_{\mathrm{EXT}} = 1 - \sum_{i=1}^{n_{\mathrm{EXT}}}(y_i - \hat{y}_i)^2 \Big/ \sum_{i=1}^{n_{\mathrm{EXT}}}(y_i - \bar{y}_{\mathrm{EXT}})^2 \qquad [3]$$

where y_i^{fit} means the fitted $\log K_D$ value of the *i*-th chemical, $\bar{y}$ stands for the average response value in the training set, y_{i} and $\hat{y}_{\mathrm{i}}$ are the observed and predicted values for the *i*-th compound, respectively. $\bar{y}_{\mathrm{EXT}}$ stands for the average response value of the validation set, *n*

stands for the number of compounds in the training set, and n_{EXT} stands for the number of compounds in the validation set.

The AD was discussed by the Williams plot of the standardized residuals and leverage values (h_i), which could be found in previous studies.[28,29,47] The leverage (h_i) value is defined as:

$$h_i = x_i^T (X^T X)^{-1} x_i \ (i = 1, \ldots, n) \quad [4]$$

$$h^* = 3(k+1)/n \quad [5]$$

where x_i stands for the descriptor vector of the considered chemical and X stands for the model matrix derived from the training set descriptor values, k is the number of predictor variables.

3. Results and discussion

3.1 Expression and purification of tumor suppressor protein p53DBD

The expression of the recombinant p53 protein showed a clear band with 53 kDa, and no soluble proteins were found in the supernatants. The recombinant protein of p53 was purified under denaturation, and the purified p53 was of high purity. The concentration of p53 protein was estimated to be 0.83 mg/L.

3.2 Binding kinetic analysis between p53 and OPFRs

For the binding interaction between OPFRs and p53 protein, it can be described by the following equation:

$$\frac{d[\mathrm{OPFR}-\mathrm{p53DBD}]}{dt} = k_a\,[\mathrm{OPFRs}][\mathrm{p53DBD}] - k_d[\mathrm{OPFR}-\mathrm{p53DBD}]$$

where k_a and k_d stand for the association rate constant and the dissociation rate constant, respectively.

The p53DBD was immobilized on gold surface and OPFRs was injected into the flow system as the analyte. The kinetic constants of the binding process were given in Table S1.

3.3 Effect of OPFRs on p53 genes and protein expression in ZF4 cell

The variation profiles of p53 mRNA expression and protein expression in ZF4 cell were shown in Figure 1. The central transcription factor p53 govers the signals arising from DNA adducts. TPP was potent inducer of expression of p53 (Figure 1B) and it also induced p53 expression at the protein level (Figure 1D). On the contrast, TCEP did not induce the expression of p53 (Figure 1A), which suggested that DNA double-strand breaks were not induced by TCEP. The lack of the p53 gene and protein expression indicated that the transcriptional genes regulating cell apoptosis, cell cycle and DNA damage were prevented from inducing.

[Insert Figure 1]

3.4 Docking analysis

The docking view of the two representative OPFRs (TCEP and TPP) in the binding site of p53 was shown in Figure 2. In the pocket of p53, His282 and Ala129 shows the important contribution of the binding interaction of chemicals. Besides, OPFRs bind with another polar region Val141.

The main interactions between the OPFRs and p53 are H-bonds and hydrophobic interactions (Figure 2). OPFRs can form hydrogen bonding as following: (i) H-bonds formed between the oxygen of TCEP and the hydrogen of Ala129 and His182, (ii) H-bonds between the hydrogen of TCEP with the carbonyl oxygen of Val141, and (ii) H-bonds between the chlorine of TCEP and phenyl hydrogen of His182 and Leu162. The three dimisional space coordinate of OPFRs in the binding domain are determined strongly by these H-bonds. There are also hydrophobic and π interactions between OPFRs and Val141, Arg181, Ile163, Ala129, His182, Ser183 in the binding sites. Figure S1 showed the electrostatic potential of the two representative OPFRs (TCEP and TPP), which suggested that the negative electrostatic potentials facilitated OPFRs to interactive with p53 easily.

[Insert Figure 2]

3.5 Molecular dynamic simulations of complexs

The MD simulations of the two OPFRs (TCEP and TPP) were carried out for 2 ns to get the minimized binding structure of OPFRs-p53. Figure 3 shows the conformational changes of OPFRs-p53 after simulation. It is indicated that there is a similar root mean square deviation (RMSD) behavior for TCEP and TPP. The superposition of the average structure of the last MD simulation and the initial docked structure is displayed in Figure S2, where the magenta and green ribbons stand for the average structure of MD simulations and the initial structure of docked binding complexes, respectively. There were no significant difference between them. The binding domain and the conformations are stabilization, which indicats that the docking results are of credit.

[Insert Figure 3]

3.6 QSAR model Development and validation

The stepwise regression was used to screen QSAR descriptors, and then 19 of them were chosen for the following model development (Table S2). They included: octanol/water partition coefficient ($\log K_{OW}$), molecular volume (V), dipole moment ($dipol$), energy of the highest occupied molecular orbital (E_{HOMO}), energy of the lowest unoccupied molecular orbital (E_{LUMO}), formal charge on the oxygen atoms of the phosphorus oxygen double bonds (q_{PO}), the most negative formal charge in the molecule (q^{-}), electrophilicity index (ω), the chemical hardness (η), the chemical potential (μ), radial distribution function -3.0/weighted by atomic van der Waals volumes (RDF_{030v}), leverage weighted autocorrelation of lag 0/weighted by mass ($HATS_{0m}$), average connectivity index chi-5 (X_{5A}), 1st component accessibility directional WHIM index/weighted by atomic Sanderson electronegativities (E_{1e}), Moran autocorrelation -lag 8/weighted by atomic van der Waals volumes ($MATS_{8v}$), Moran

autocorrelation -lag 8/weighted by atomic Sanderson electronegativities ($MATS_{8e}$), Moran autocorrelation -lag7/weighted by atomic van der Waals volumes ($MATS_{7v}$), signal 17/weighted by atomic masses (Mor_{17m}), and radial distribution function -3.5/ weighted by atomic masses (RDF_{035m}).

[Insert Table S2]

The developed optimal QSAR model by PLS analysis is:

$$\log K_D = -4.76 + 5.67\times10^{-1}X_{5A} + 7.15\times10^{-1}MATS_{7v} + 1.67Mor_{17m}$$

$$n \text{ (training set)} = 7,\ A = 2,\ R^2 = 0.892,\ Q^2_{CUM} = 0.743,\ RMSE = 0.238 \text{ (training set)},$$

$$n \text{ (validation set)} = 3,\ Q^2_{EXT} = 0.647,\ RMSE = 0.338 \text{ (validation set)},$$

$$\text{significance level } (p) < 0.001$$

Table 1 listed the predicted $\log K_D$ values and residuals for the OPFRs. The R^2 was 0.892, which indicated the QSAR model was of good goodness-of-fit. Q^2_{CUM} is as high as 0.743, which showed the QSAR model had good robustness. The differences between Q^2_{CUM} and R^2 is 0.149, which indicated there was no over-fitting in the model.[48] The predicted $\log K_D$ values were in accordance with the observed values for both the validation and training sets (Figure 4). The QSAR model was of receivable predictive ability with $Q^2_{EXT} = 0.647$, $RMSE = 0.338$. Therefore, the current QSAR model showed famous performance.

[Insert Table 1]

[Insert Figure 4]

3.7 Applicability domain

As shown in Figure S3, the distribution of residuals is tested by Kolmogorov-Smirnov test for normality ($p < 0.05$), which indicated that the residuals are non-systematic and normal distribution. Then, the AD of the developed QSAR model can be visualized by the Williams plot. As shown in the Figure 5, OPFRs in the training and validation sets were found with $h_i < h^*$ ($h^* = 1.71$) and they were in the domain. There were also no outliers for the QSAR model.

[*Insert Figure 5*]

3.8 Mechanistic implications

The values of the variable importance in the projection (*VIP*) and PLS weights (W^*) are listed in Table 2. The two PLS components were extracted which loaded on $Mor_{17\mathrm{m}}$, $MATS_{7\mathrm{v}}$ and $X_{5\mathrm{A}}$.

[*Insert Table 2*]

$Mor_{17\mathrm{m}}$ is a 3D-MoRSE descriptors, and it shows the three dimensional structure of compound weighted by atomic masses.[49] The *VIP* value of $Mor_{17\mathrm{m}}$ is the largest among the three descriptors, which shows $Mor_{17\mathrm{m}}$ remarkably governs $\log K_D$. $MATS_{7\mathrm{v}}$ is weighted by atomic van der Waals volumes, belonging to 2D autocorrelation descriptor.[50] The $X_{5\mathrm{A}}$ is average connectivity index, which shows the topological characteristics in the developed QSAR model. It can descript the binding interactions and the molecular affect between the OPFRs compounds and p53. The coefficients in the current QSAR model showed that the selected descriptors ($Mor_{17\mathrm{m}}$, $MATS_{7\mathrm{v}}$ and $X_{5\mathrm{A}}$) were positively correlated with the $\log K_D$ values.

Because $Mor_{17\mathrm{m}}$ correlates with $\log K_{\mathrm{OW}}$ (r = 0.502) positively, then the results are comprehensible. The OPFRs compounds with large $\log K_{\mathrm{OW}}$ values may distribute into the biophase easily. Likewise, $Mor_{17\mathrm{m}}$ correlates with q^- (r = 0.698) negatively. q^- can express the the basicity of hydrogen bond for a chemicals, and itself is negative.[36] From docking analysis, H-bonds were found to be the significant interaction between OPFRs and p53. The OPFRs with smaller q^- values may have bigger hydrogen bond basicity, and accordingly it can easy to form hydrogen bonding and exhibit strong binding affinities.

4. Conclusions

The binding affinities of 10 OPFRs to the recombinant zebrafish p53 protein were determined by SPR. OPFRs could induce the expression of p53 mRNA and protein.

Molecular docking and dynamics simulation simulations suggested that H-bonds and electrostatic interactions are of great importance on the binding interactions between OPFRs and p53. The QSAR model was developed to descript the binding affinities and found the mechanism of action. The OPFRs with higher ability to form H-bonding with the p53, exhibiting high binding affinity. The developed QSAR model are of good robustness, predicability and mechanism interpretability.

Funding Sources

This research was supported by the National Natural Science Foundation of China (21107136) and the International Foundation for Science (F/5230-1).

Abbreviations

1. OPFRs: organophosphate flame retardants
2. TCEP: Tris(2-chloroethyl)phosphate
3. TCPP: Tris(2-chloroisopropyl)phosphate
4. TPP: triphenyl phosphate
5. DnBP: Di-n-butylphosphate
6. TEHP: Tris(2-ethylhexyl)phosphate
7. TPhP: Triphenylphosphate
8. TEP: Triethylphosphate
9. TMP: Trimethylphosphate
10. TCrP: Tricresyl phosphate
11. TnBP: tri-n-butylphosphate
12. TiBP: tri-iso-butylphosphate
13. TPrP: tri-n-propylphosphate
14. TBEP: tris-(butoxyethyl)-phosphate
15. AD: applicability domain

16. E_{HOMO}: energy of the highest occupied molecular orbital

17. E_{LUMO}: energy of the lowest unoccupied molecular orbital

18. $\log K_{OW}$: logarithm of octanol/water partition coefficient

19. PLS: partial least squares

20. Q^2_{CUM}: the fraction of the total variation of the dependent variables that can be predicted by all the extracted components

21. QSAR: quantitative structure-activity relationship

22. R: determination coefficient

23. $RMSE$: root mean square error

24. MD: molecular dynamics

Supporting Information

The association rate constant (k_a), the dissociationrate constant (k_d), the binding constant (K_D) and the binding energy ($E_{binding}$) for 10 organophosphate flame retardants (OPFRs), molecular descriptors in the developed QSAR model, the electrostatic potential of the two representative OPFRs (TCEP and TPP) and the superimposition of the average structure from the last MD simulation. This material is available free of charge via the Internet at http://pubs.acs.org.

Rerference

(1) Dishaw, L. V., Powers, C. M., Ryde, I. T., Roberts, S. C., Seidler, F. J., Slotkin, T. A., and Stapleton, H. M. (2011) Is the PentaBDE replacement, tris (1,3-dichloropropyl) phosphate (TDCPP), a developmental neurotoxicant? Studies in PC12 cells. *Toxicol. Appl. Pharm. 256*, 281-289.

(2) Marklund, A., Andersson, B., and Haglund, P. (2003) Screening of organophosphorus compounds and their distribution in various indoor environments. *Chemosphere 53*, 1137-1146.

(3) Reemtsma, T., Quintana, J. B., Rodil, R., Garcia-Lopez, M., and Rodriguez, I. (2008) Organophosphorus flame retardants and plasticizers in water and air I. Occurrence and fate. *Trac-Trend. Anal. Chem. 27*, 727-737.

(4) Andresen, J. A., Grundmann, A., and Bester, K. (2004) Organophosphorus flame retardants and plasticisers in surface waters. *Sci. Total Environ.* 332, 155-166.

(5) Hartmann, P. C., Burgi, D., and Giger, W. (2004) Organophosphate flame retardants and plasticizers in indoor air. *Chemosphere 57*, 781-787.

(6) Stapleton, H. M., Klosterhaus, S., Eagle, S., Fuh, J., Meeker, J. D., Blum, A., and Webster, T. F. (2009) Detection of organophosphate flame retardants in furniture foam and US house dust. *Environ. Sci. Technol. 43*, 7490-7495.

(7) Takigami, H., Suzuki, G., Hirai, Y., Ishikawa, Y., Sunami, M., and Sakai, S. (2009) Flame retardants in indoor dust and air of a hotel in Japan. *Environ. Int. 35*, 688-693.

(8) Bacaloni, A., Cucci, F., Guarino, C., Nazzari, M., Samperi, R., and Lagana, A. (2008) Occurrence of organophosphorus flame retardant and plasticizers in three volcanic lakes of Central Italy. *Environ. Sci. Technol. 42*, 1898-1903.

(9) Regnery, J., and Puttmann, W. (2010) Occurrence and fate of organophosphorus flame retardants and plasticizers in urban and remote surface waters in Germany. *Water Res. 44*, 4097-4104.

(10) Garcia-Lopez, M., Rodriguez, I., and Cela, R. (2009) Pressurized liquid extraction of organophosphate triesters from sediment samples using aqueous solutions. *J. Chromatogr. A 1216*, 6986-6993.

(11) David, M. D., and Seiber, J. N. (1999) Analysis of organophosphate hydraulic fluids in US Air Force base soils. *Arch. Environ. Con. Tox. 36*, 235-241.

(12) Yasuhara, A., Shiraishi, H., Nishikawa, M., Yamamoto, T., Nakasugi, O., Okumura, T., Kenmotsu, K., Fukui, H., Nagase, M., and Kawagoshi, Y. (1999) Organic components in

leachates from hazardous waste disposal sites. *Waste Manage. Res. 17*, 186-197.

(13) Liu, X., Ji, K., and Choi, K. (2012) Endocrine disruption potentials of organophosphate flame retardants and related mechanisms in H295R and MVLN cell lines and in zebrafish. *Aquat. Toxicol. 114*, 173-181.

(14) Martinez-Carballo, E., Gonzalez-Barreiro, C., Sitka, A., Scharf, S., and Gans, O. (2007) Determination of selected organophosphate esters in the aquatic environment of Austria. *Sci. Total Environ. 388*, 290-299.

(15) Matthews, H. B., Dixon, D., Herr, D. W., and Tilson, H. (1990) Subchronic toxicity studies indicate that tris(2-chloroethyl)phosphate administration results in lesions in the rat hippocampus. *Toxicol. Ind. Health 6*, 1-15.

(16) Commission, E. European Chemicals Bureau. IUCLID, dataset tris(2-chloromethyl) phosphate, EINECS No. 204-118-5; . http://ecb.jrc.it/ESIS. 2001.

(17) Saboori, A. M., Lang, D. M., and Newcombe, D. S. (1991) Structural requirements for the inhibition of human monocyte carboxylesterase by organophosphorus compounds. *Chem.-Biol. Interact. 80*, 327-338.

(18) Meeker, J. D., and Stapleton, H. M. (2010) House dust concentrations of organophosphate flame retardants in relation to hormone levels and semen quality parameters. *Environ. Health Perspect. 118*, 318-323.

(19) Grunwald, J. D., and Eisen, J. S. (2002). Timeline: Headwaters of the zebrafish - emergence of a new model vertebrate. *Nat. Rev. Genet. 3*, 717–724.

(20) Robert G. (2003). Zebra fish: An uncharted behavior genetic model. *Behav. Genet. 33*, 461-468.

(21) Howe, K. ,Clark, M.D., Torroja, C.F., Torrance, J., Berthelot, C., Muffato, M., Collins, J.E., Humphray, S., McLaren, K., Matthews, L., McLaren, S., Sealy, I., Caccamo, M., Churcher, C., Scott, C., Barrett, J.C., Koch, R., Rauch, G.J, White, S., Chow, W., Kilian,

B., Quintais, L.T., Guerra-Assuncao, J.A, Zhou, Y., Gu, Y., Yen, J., Vogel, J.H., Eyre, T., Redmond, S., Banerjee, R., Chi, J.X., Fu, B.Y., Langley, E., Maguire, S.F., Laird, G.K., Lloyd, D., Kenyon, E., Donaldson, S., Sehra, H., Almeida-King, J., Loveland, J., Trevanion, S., Jones, M., Quail, M., Willey, D., Hunt, A., Burton, J., Sims, S., McLay, K., Plumb, B., Davis, J., Clee, C., Oliver, K., Clark, R., Riddle, C., Eliott, D., Threadgold, G., Harden, G., Ware, D., Mortimer, B., Kerry, G., Heath, P., Phillimore, B., Tracey, A., Corby, N., Dunn, M., Johnson, C., Wood, J., Clark, S., Pelan, S., Griffiths, G., Smith, M., Glithero, R., Howden, P., Barker, N., Stevens, C., Harley, J., Holt, K., Panagiotidis, G., Lovell, J., Beasley, H., Henderson, C., Gordon, D., Auger, K., Wright, D., Collins, J., Raisen, C., Dyer, L., Leung, K., Robertson, L., Ambridge, K., Leongamornlert, D., McGuire, S., Gilderthorp, R., Griffiths, C., Manthravadi, D., Nichol, S., Barker, G., Whitehead, S., Kay, M., Brown, J., Murnane, C., Gray, E., Humphries, M., Sycamore, N., Barker, D., Saunders, D., Wallis, J., Babbage, A., Hammond, S., Mashreghi-Mohammadi, M., Barr, L., Martin, S., Wray, P., Ellington, A., Matthews, N., Ellwood, M., Woodmansey, R., Clark, G., Cooper, J., Tromans, A., Grafham, D., Skuce, C., Pandian, R., Andrews, R., Harrison, E., Kimberley, A., Garnett, J., Fosker, N., Hall, R., Garner, P., Kelly, D., Bird, C., Palmer, S., Gehring, I., Berger, A., Dooley, C.M., Ersan-Urun, Z., Eser, C., Geiger, H., Geisler, M., Karotki, L., Kirn, A., Konantz, J., Konantz, M., Oberlander, M., Rudolph-Geiger, S., Teucke, M., Osoegawa, K., Zhu, B.L., Rapp, A., Widaa, S., Langford, C., Yang, F.T., Carter, N.P., Harrow, J., Ning, Z.M., Herrero, J., Searle, S.M.J., Enright, A., Geisler, R., Plasterk, R.H.A., Lee, C., Westerfield, M., de Jong, P.J., Zon, L.I., Postlethwait, J.H., Nusslein-Volhard, C., Hubbard, T.J.P., Crollius, H.R., Rogers, J., and Stemple, D.L. (2013) The zebrafish reference genome sequence and its relationship to the human genome. *Nature 496*, 498-503.

(22) Vogelstein, B., Lane, D., and Levine, A. J. (2000) Surfing the p53 network. *Nature 408*,

307-310.

(23) Di Agostino, S., Strano, S., Emiliozzi, V., Zerbini, V., Mottolese, F., Sacchi, A., Blandino, G., and Piaggio, G. (2006) Gain of function of mutant p53: The mutant p53/NF-Y protein complex reveals an aberrant transcriptional mechanism of cell cycle regulation. *Cancer Cell 10*, 191-202.

(24) Niu, J.F., Lin, H., Gong, C., and Sun X.M. (2013) Theoretical and experimental insights into the electrochemical mineralization mechanism of perfluorooctanoic acid. *Environ. Sci. Technol. 47*, 14341–14349.

(25) Niu. J.F., Shen, Z.Y., Yang, Z.F., Long, X.X., and Yu, G. (2006) Quantitative structure-property relationships on photodegradation of polybrominated diphenyl ethers. *Chemosphere 64*, 658-665.

(26) OECD. (2007) Guidance document on the validation of (Quantitative) Structure-Activity Relationships [(Q)SARs] models. Available online at: http://appli1.oecd.org/olis/2007doc.nsf/linkto/env-jm-mono(2007)2.

(27) Martinez, L., Polikarpov, I., and Skaf, M. S. (2008) Only subtle protein conformational adaptations are required for ligand binding to thyroid hormone receptors: Simulations using a novel multipoint steered molecular dynamics approach. *J. Phys. Chem. B 112*, 10741-10751.

(28) Li, F., Xie, Q., Li, X. H., Li, N., Chi, P., Chen, J. W., Wang, Z. J., and Hao, C. (2010) Hormone activity of hydroxylated polybrominated diphenyl ethers on human thyroid receptor β : *in vitro* and *in silico* investigations. *Environ. Health Perspect. 118*, 602-606.

(29) Li, F., Li, X. H., Shao, J. P., Chi, P., Chen, J. W., and Wang, Z. J. (2010) Estrogenic activity of anthraquinone derivatives: *in vitro* and *in silico* studies. *Chem. Res. Toxicol. 23*, 1349-1355.

(30) Li, F., Wu, H. F., Li, L. Z., Li, X. H., Zhao, J. M., and Peijnenburg, W. J. G. M. (2012)

Docking and QSAR study on the binding interactions between polycyclic aromatic hydrocarbons and estrogen receptor. *Ecotoxicol. Environ. Saf. 80*, 273-279.

(31) Sipova, H., and Homola, J. (2013) Surface plasmon resonance sensing of nucleic acids: A review. *Anal. Chim. Acta 773*, 9-23.

(32) Karlsson, R. (2004) SPR for molecular interaction analysis: a review of emerging application areas. *J. Mol. Recognit. 17*, 151-161.

(33)Campbell, K., Huet, A. C., Charlier, C., Higgins, C., Delahaut, P., and Elliott, C. T. (2009) Comparison of ELISA and SPR biosensor technology for the detection of paralytic shellfish poisoning toxins. *J. Chromatogr. B: Anal. Technol. Biomed. Life Sci. 877*, 4079-4089.

(34) Xue, Y. L., Wang, S. A., and Feng, X. Z. (2009) Effect of metal ion on the structural stability of tumour suppressor protein p53 DNA-binding domain. *J. Biochem. 146*, 193-200.

(35) Katayama, M., Sato, T., and Kuromitsu, J. (2012) Capture molecules preconditioned for kinetic analysis of high-affinity antigen-antibody complex in Biacore A100. *Anal. Biochem. 424*, 168-177.

(36) Drake, A. W., Tang, M. L., Papalia, G. A., Landes, G., Haak-Frendscho, M., and Klakamp, S. L. (2012) Biacore surface matrix effects on the binding kinetics and affinity of an antigen/antibody complex. *Anal. Biochem. 429*, 58-69.

(37) Livak, K. J.; Schmittgen, T. D. (2001) Analysis of relative gene expression data using real-time quantitative PCR and the 2(T)(-Delta Delta C) method. *Methods 25*, 402-408.

(38) Wu, G. S., Robertson, D. H., Brooks, C. L., and Vieth, M. (2003) Detailed analysis of grid-based molecular docking: A case study of CDOCKER - A CHARMm-based MD docking algorithm. *J. Comput. Chem. 24*, 1549-1562.

(39) Nguyen, T. H., Goss, K. U., and Ball, W. P. (2005) Polyparameter linear free energy

relationships for estimating the equilibrium partition of organic compounds between water and the natural organic matter in soils and sediments. *Environ. Sci. Technol. 39*, 913-924.

(40) Colosi, L. M., Huang, Q. G., and Weber, W. J. (2006) Quantitative structure-activity relationship based quantification of the impacts of enzyme-substrate binding on rates of peroxidase-mediated reactions of estrogenic phenolic chemicals. *J. Am. Chem. Soc. 128*, 4041-4047.

(41) Frisch, M. J., Trucks, G. W., Schlegel, H. B., Scuseria, G. E., Robb, M. A., Cheeseman, J. R., Scalmani, G., Barone, V., Mennucci, B., Petersson, G. A., Nakatsuji, H., Caricato, M., Li, X., Hratchian, H. P., Izmaylov, A. F., Bloino, J., Zheng, G., Sonnenberg, J. L., Hada, M., Ehara, M., Toyota, K., Fukuda, R., Hasegawa, J., Ishida, M., Nakajima, T., Honda, Y., Kitao, O., Nakai, H., Vreven, T., Montgomery, Jr., J. A., Peralta, J. E., Ogliaro, F., Bearpark, M., Heyd, J. J., Brothers, E., Kudin, K. N., Staroverov, V. N., Kobayashi, R., Normand, J., Raghavachari, K., Rendell, A., Burant, J. C. Iyengar, S. S. Tomasi, J. Cossi, M. Rega, Millam, N. J., Klene, M. Knox, J. E., Cross, J. B., Bakken, V., Adamo, C., Jaramillo, J., Gomperts, R. E. Stratmann, O. Yazyev, A. J. Austin, R. Cammi, C. Pomelli, J. W. Ochterski, R. Martin, R. L., Morokuma, K., Zakrzewski, V. G., Voth, G. A., Salvador, P., Dannenberg, J. J., Dapprich, S., Daniels, A. D., Farkas, O., Foresman, J. B., Ortiz, J. V., Cioslowski, J., and Fox, D. J. (2009) Gaussian 09, Revision A.1. Gaussian, Inc., Wallingford CT.

(42) Arulmozhiraja, S., Shiraishi, F., Okumura, T., Iida, M., Takigami, H., Edmonds, J. S., and Morita, M. (2005) Structural requirements for the interaction of 91 hydroxylated polychlorinated biphenyls with estrogen and thyroid hormone receptors. *Toxicol. Sci. 84*, 49-62.

(43) Huetz, P., Kamarulzaman, E. E., Wahab, H. A., and Mavri, J. (2004) Chemical reactivity

as a tool to study carcinogenicity: Reaction between estradiol and estrone 3,4-quinones ultimate carcinogens and guanine. *J. Chem. Inf. Comput. Sci. 44*, 310-314.

(44) Todeschini, R., and Consonni, V. (2000) Handbook of molecular descriptors. Wiley-VCH, Weinheim, Germany.

(45) Wold, S., Sjostrom, M., and Eriksson, L. (2001) PLS-regression: a basic tool of chemometrics. *Chemom. Intell. Lab. Syst. 58*, 109-130.

(46) Schuurmann, G., Ebert, R. U., Chen, J. W., Wang, B., and Kuhne, R. (2008) External validation and prediction employing the predictive squared correlation coefficient - test set activity mean vs training set activity mean. *J. Chem. Inf. Comput. Sci. 48*, 2140-2145.

(47) Eriksson, L., Jaworska, J., Worth, A. P., Cronin, M. T. D., McDowell, R. M., and Gramatica, P. (2003) Methods for reliability and uncertainty assessment and for applicability evaluations of classification- and regression-based QSARs. *Environ. Health Perspect. 111*, 1361-1375.

(48) Golbraikh, A., and Tropsha, A. (2002) Beware of q^2! *J. Mol. Graph. Model. 20*, 269-276.

(49) Gasteiger, J., Sadowski, J., Schuur, J., Selzer, P., Steinhauer, L., and Steinhauer, V. (1996) Chemical information in 3D space. *J. Chem. Inf. Comput. Sci. 36*, 1030-1037.

(50) Roy, N., and Kadam, R. U. (2006) Cluster analysis and two-dimensional quantitative structure-activity relationship (2D-QSAR) of Pseudomonas aeruginosa deacetylase LpxC inhibitors. *Bioorg. Med. Chem. Lett. 16*, 5136-5143.

533 Table 1 Logarithm of the observed and predicted dissociation constant (logK_D) of the
534 considered compounds.

No.	Compounds	logK_D		
		Observed	Predicted	Residuals
1	TCEP	-5.55	-5.32	-0.24
2	TCPP	-5.02	-5.03	0.01
3	TPrP*	-5.55	-5.28	-0.27
4	DnBP*	-4.84	-5.01	0.17
5	TEHP	-6.34	-6.34	-0.01
6	TBEP	-5.06	-5.43	0.37
7	TPhP	-4.15	-4.31	0.16
8	TEP*	-4.92	-4.99	0.07
9	TnBP	-5.10	-4.86	-0.24
10	TCrP	-5.14	-5.05	-0.09

535 * Compounds in the validation set.

Table 2 *VIP* values and PLS weights for the optimal PLS model.

	VIP	$W^*c[1]$	$W^*c[2]$
Mor_{17m}	1.35	0.88	0.82
$MATS_{7v}$	0.81	-0.31	0.59
X_{5A}	0.71	-0.36	0.37

Figure Caption

Figure 1 Induction of expression of p53 in the ZF4 cells after exposure to different concentrations of TCEP and TPP, respectively. (A) Modulation of levels of p53 mRNA by TCEP and TPP. Total RNA was isolated and quantitative RT-PCR carried out for the detection of levels of p53. Data were normalized to expression of the β-actin housekeeping gene. Results are means ± S.D. of two independent experiments each carried out in triplicate. (B) Induction of p53 proteins. Cells were treated with the indicated concentrations of TCEP and TPP or DMSO (solvent control) for 24 h. Cell lysates were prepared as described in section 2.3 and analyzed by western blotting of levels of p53 and β-actin protein (loading control). ** $p < 0.01$.

Figure 2 Hydrogen bondings (left) and hydrophobic interactions (right) for TCEP or TPP in the binding site of p53.

Figure 3 The RMSD of the backbone atoms of both complexes during MD simulations.

Figure 4 Plot of observed versus predicted $\log K_D$ values for the training and validation.

Figure 5 Plot of standardized residuals versus leverages. Dash lines represent ±3 standardized residual, dotted line represents warning leverage ($h^* = 1.71$).

Figure 1

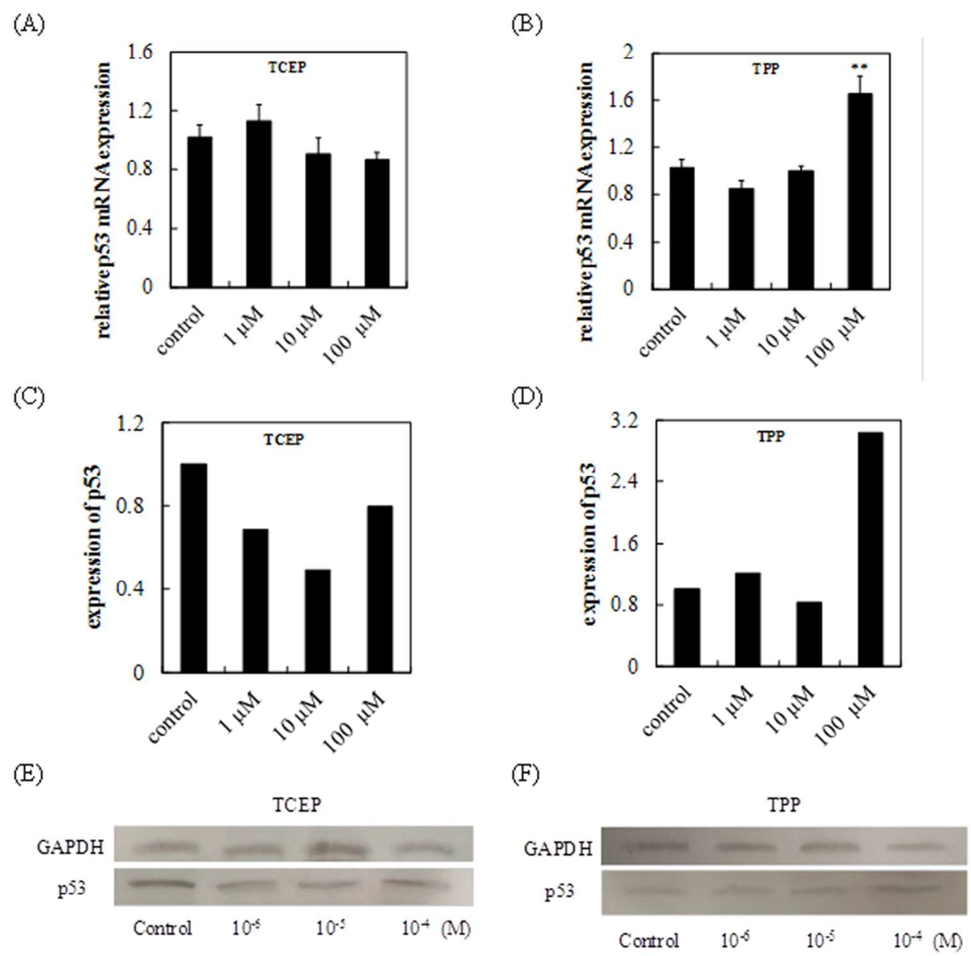

Induction of expression of p53 in the ZF4 cells after exposure to different concentrations of TCEP and TPP, respectively.
99x104mm (300 x 300 DPI)

Figure 2

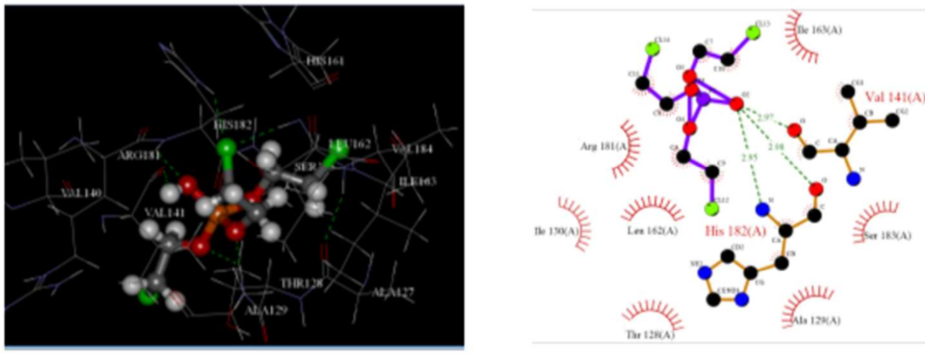

(a) Tris(2-chloroethyl)phosphate

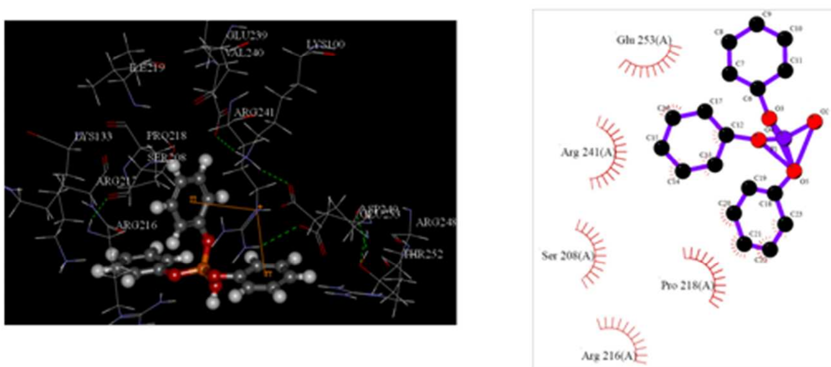

(b) Triphenyl phosphate

ligand bond receptor bond Hydrogen bond receptor residues involved in hydrophobic interactions Corresponding atoms involved in hydrophobic interactions.

Hydrogen bondings (left) and hydrophobic interactions (right) for TCEP or TPP in the binding site of p53.
99x113mm (300 x 300 DPI)

Figure 3

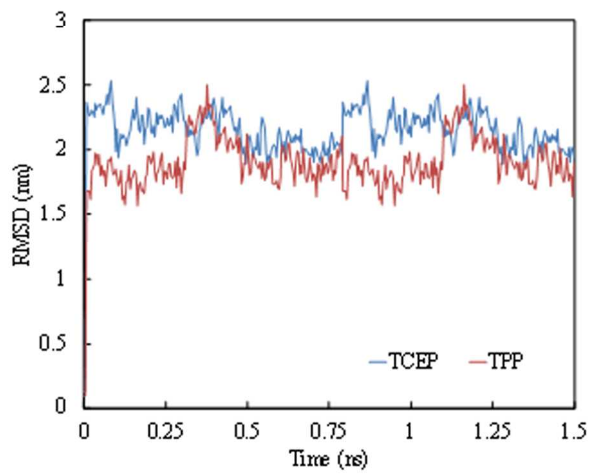

The RMSD of the backbone atoms of both complexes during MD simulations.
99x55mm (300 x 300 DPI)

Figure 4

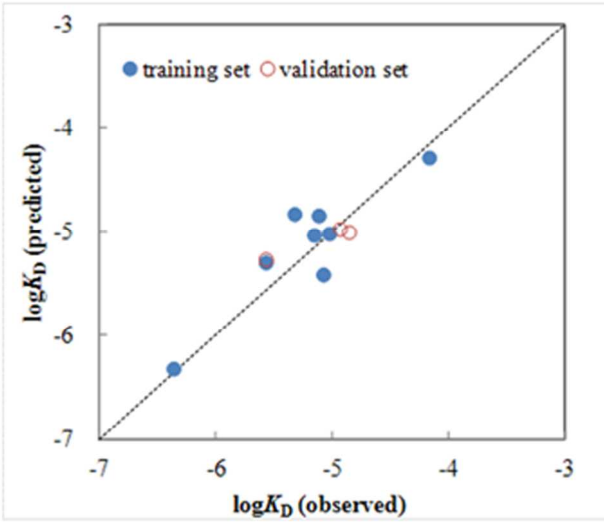

Plot of observed versus predicted logKD values for the training and validation.
99x59mm (300 x 300 DPI)

Figure 5

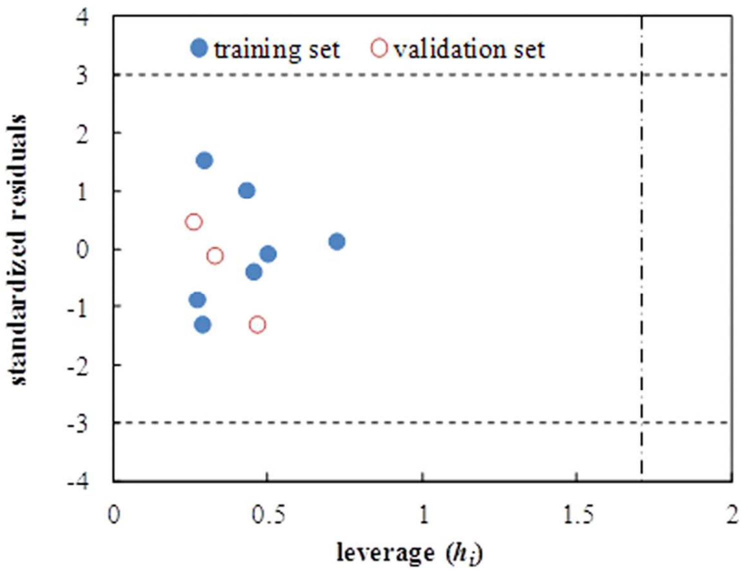

Plot of standardized residuals versus leverages. Dash lines represent ±3 standardized residual, dotted line represents warning leverage (h* = 1.71).
99x66mm (300 x 300 DPI)